



# Effect of train dynamics on seismic response of steel monorail bridges under moderate ground motion

Kim, Chul-Woo

Kawatani, Mitsuo

---

**(Citation)**

Earthquake Engineering & Structural Dynamics, 35(10):1225-1245

**(Issue Date)**

2006-08

**(Resource Type)**

journal article

**(Version)**

Accepted Manuscript

**(Rights)**

This is a preprint of an article published in [Earthquake Engineering & Structural Dynamics, vol.35(10), 200608, p.1225 - 1245, Wiley]

**(URL)**

<https://hdl.handle.net/20.500.14094/90000472>



# **Effect of train dynamics on seismic response of steel monorail bridges under moderate ground motion**

**Chul-Woo Kim<sup>\*1</sup>, Mitsuo Kawatani<sup>2</sup>**

*Department of Civil Engineering, Kobe University, 1-1 Rokkodai, Nada, Kobe 657-8501, Japan*

## **SUMMARY**

This study is intended to investigate the seismic response of steel monorail bridges using three-dimensional dynamic response analysis. We particularly consider monorail bridge-train interaction when subjected to ground motion that occurs with high probability. A monorail train car with two bogies with pneumatic tires for running, steering and stabilizing wheels is assumed to be represented sufficiently by a discrete rigid multi-body system with 15 degrees of freedom (DOFs). Bridges are considered as an assemblage of beam elements with 6 DOFs at each node. Modal analysis is used for dynamic response analysis under moderate earthquakes. The seismic response of an advanced monorail bridge that adopts a simplified structural system and composite girders is investigated through comparison with seismic responses of a conventional bridge. The acceleration response of a monorail train is also calculated to investigate the effect of structural types of bridges on the train's dynamic response during earthquakes. Results show that the seismic responses of the advanced bridges are greater than those of the conventional monorail bridge because of the simplified structural system and increased girder weight that is attributable to composite girders of the advanced bridge. Moreover, the train on the advanced bridge shows greater dynamic response than that on the conventional bridge. Observations reveal that the dynamic monorail train system acts as a damper on the monorail bridge. That fact shows that the existing design, which considers a train as additional mass, yields a conservative result.

KEY WORDS: bridge-train interaction; seismic response; three-dimensional analysis; monorail bridge

---

<sup>\*</sup>Correspondence to: Chul-Woo Kim, Department of Civil Engineering, Kobe University, 1-1 Rokkodai, Nada, Kobe 657-8501, Japan. Phone: +81-78-803-6383; FAX: +81-78-803-6069.

<sup>1</sup> E-mail: cwkim@kobe-u.ac.jp

<sup>2</sup> E-mail: m-kawa@kobe-u.ac.jp

<sup>1</sup> COE Researcher

<sup>2</sup> Professor

## INTRODUCTION

Traffic problems in major cities of the world during the last two decades have emphasized the considerable need for new transportation systems. Straddle-type monorail systems (Figure 1) have been adopted for new transportation systems throughout Japan in the cities of Tokyo, Osaka, Tama, Kita-Kyushu, and Naha. Cost-efficiency is another important issue in modern bridge design. That situation has stimulated structural engineers to create a concept of rationalized design strategy, even for monorail bridges. Therefore, a new type of steel-concrete composite bridge for monorails (hereafter, advanced bridge) has been developed in Japan. A simplified lateral bracing system in the advanced bridge constitutes the major difference from conventional bridges. The composite steel girder with an RC tramway is another advanced concept to enhance braking performance of monorail trains, even though it makes the advanced bridge heavier than a conventional bridge. Actually, the authors have described in a recent report [1] that advanced bridges are affected more easily by lateral loading effects than conventional bridges under a moving train. That fact, together with the advanced scheme described above, suggests that the simplified lateral bracing system and the composite track girder might engender problems related to seismic performance of the bridge.

Performance-based seismic design of bridges is an issue of great concern in countries, such as Japan, which are located in earthquake-prone regions. The magnitude 6.6 earthquake that struck Niigata Prefecture on the evening of 23 October 2004 was the most damaging earthquake to affect Japan since the 1995 Kobe earthquake. Roads, railways and other lifelines were compromised, engendering major economic disruption. One Joetsu Shinkansen train that crosses this region in a north/south direction and terminates in Niigata city was derailed just south of Nagaoka city by the earthquake. That event was, in itself, an unprecedented shock to the civil engineering community.

In contrast to the railway system, the straddle-type monorail train employs steering and stabilizing wheels that firmly grasp the track girder of monorail bridges. Consequently, the lateral motion and rolling of a monorail train can affect the dynamic response of the bridge [2]. The live load attributable to the weight of the monorail train plays an important role in the seismic design of monorail bridges because of the large load of the train's weight compared with the dead load of bridges. The dynamic system of the monorail train is an important factor in the seismic response of the monorail bridge because the train has a complicated dynamic system.

One question remaining to be answered is: What is the seismic behavior of the monorail bridges considering bridge-train interaction when subjected to earthquakes? Another pertinent question is: What is the difference of the seismic responses of conventional and advanced bridges?

Rather limited efforts have been devoted to the effects of train dynamics on the seismic resistance of bridges, but some interesting studies have explored dynamic stability of railway trains and other vehicles with ground motion. Kameda *et al.* [3] investigated the effect of vehicle loading on seismic responses of highway bridges. That study concluded that the seismic response of the bridge can increase or decrease according to the phase difference between the vehicle and bridge systems. Yang and Wu [4] investigated the

dynamic stability of trains moving over bridges that were shaken by an earthquake. Some studies have examined dynamic stability of trains or other vehicles under seismic motions without considering interaction with bridge structures. Miyamoto et al. [5] estimated the running safety of trains under earthquakes on the condition that the train is set as stationary on the track. Maruyama and Yamazaki [6] performed a seismic response analysis on the stability of running vehicles. However, few studies have addressed the seismic response of the monorail bridge incorporating the bridge-train interactive effect.

This study is an attempt to investigate the seismic behavior of conventional and advanced monorail bridges with steel piers incorporating interaction between bridges and trains under moderate ground motions (called Level-I) by means of a three-dimensional dynamic response analysis. The Level-I ground motions specified in the Design Specification of Highway Bridges of the Japan Road Association (hereafter, JRA code) [7] are used as moderate ground motions that occur with high probability. As for the seismic performance level under moderate ground motion, it is assumed that both important and standard bridges should behave in an elastic manner without important damage under the Level-I ground motion according to the JRA code.

## **DYNAMIC EQUATIONS OF MONORAIL BRIDGE-TRAIN INTERACTION WITH EARTHQUAKE**

Finite element (FE) method is used as a tool for idealizing bridges. Bridges are considered as an assemblage of beam elements with six degrees of freedom (DOFs) at each node. Modal analysis is adopted for dynamic response analysis under moderate earthquakes. The consistent mass system and Rayleigh damping are used respectively to form the mass and damping matrices of the bridge model. A process known as Guyan reduction [8] is used to improve the efficiency of calculation.

### *Train model*

A monorail train car has two bogies with pneumatic tires for running, steering and stabilizing wheels. The car's dynamic behavior is assumed to be sufficiently represented by a discrete rigid multi-body system with 15 DOFs, as shown in Figure 2, where  $m$  indicates the mass,  $K$  is the spring constant,  $C$  is the damping coefficient, and  $Z$ ,  $Y$  and  $\theta$  respectively indicate the vertical, lateral and rotational displacement. Details of the notation and dynamic characteristics of the monorail train are summarized in Table I.

The equations of motion for a car in the train can be derived using Lagrange's formulation as

$$\frac{\partial}{\partial t} \left( \frac{\partial T}{\partial \dot{a}_i} \right) - \frac{\partial T}{\partial a_i} + \frac{\partial U_e}{\partial a_i} + \frac{\partial U_d}{\partial \dot{a}_i} = 0, \quad (1)$$

where  $T$  is the kinetic energy,  $U_e$  is the potential energy of the system and  $U_d$  is the dissipation energy attributable to damping of the system;  $a_i$  is a generalized coordinate.

Modifying the energy equations for vehicles on a highway bridge [9] develops the kinetic energy, potential energy and dissipation energy of the monorail car on a bridge. These are expressed as a set of generalized coordinates as the following [2].

$$T = \frac{1}{2} \sum_{v=1}^{nv} \left[ m_{v11} \dot{Z}_{v11}^2 + m_{v11} \dot{Y}_{v11}^2 + I_{vx11} \dot{\theta}_{vx11}^2 + I_{vy11} \dot{\theta}_{vy11}^2 + I_{vz11} \dot{\theta}_{vz11}^2 + \sum_{i=1}^2 \left\{ m_{v2i} \dot{Z}_{v2i}^2 + m_{v2i} \dot{Y}_{v2i}^2 + I_{vx2i} \dot{\theta}_{vx2i}^2 + I_{vy2i} \dot{\theta}_{vy2i}^2 + I_{vz2i} \dot{\theta}_{vz2i}^2 \right\} \right] \quad (2)$$

$$U_e = \frac{1}{2} \sum_{v=1}^{nv} \left[ \sum_{i=1}^2 \sum_{j=1}^2 \sum_{n=1}^2 \left\{ K_{vi1jn} R_{vi1jn}^2 \delta_{1j} + K_{vi2jn} R_{vi2jn}^2 + K_{vi3jn} R_{vi3jn}^2 + K_{vi4jn} R_{vi4jn}^2 \delta_{1j} \right\} + \sum_{i=1}^2 K_{vi511} R_{vi511}^2 \right] \quad (3)$$

$$U_d = \frac{1}{2} \sum_{v=1}^{nv} \left[ \sum_{i=1}^2 \sum_{j=1}^2 \sum_{n=1}^2 \left\{ C_{vi1jn} \dot{R}_{vi1jn}^2 \delta_{1j} + C_{vi2jn} \dot{R}_{vi2jn}^2 + C_{vi3jn} \dot{R}_{vi3jn}^2 + C_{vi4jn} \dot{R}_{vi4jn}^2 \delta_{1j} \right\} + \sum_{i=1}^2 C_{vi511} \dot{R}_{vi511}^2 \right] \quad (4)$$

In those equations,  $nv$  is the number of cars in monorail train,  $I$  is the mass moment of inertia,  $R_{vimjn}$  is the relative displacement at springs and dampers, and  $\delta_{ij}$  is Kronecker's delta. The subscript  $v$  indicates the number of monorail cars on the bridge. Subscript  $i$  is an index indicating the suspension position of a car of monorail train ( $i=1$  and  $2$  are the front and rear suspensions, respectively). Subscript  $j$  is the tire position in a bogie (e.g.  $j=1$  and  $2$  are the front and rear tires of the bogie system, respectively). In addition,  $n$  is an index indicating either the left or right side of the train.

The relative displacement is definable in the following manner.

$$R_{vi1jn} = Z_{v11} - Z_{v2i} + (-1)^n \theta_{vx11} \lambda_{vy2} - (-1)^n \theta_{vx2i} \lambda_{vy2} - (-1)^i \theta_{vy11} \lambda_{vxi} \quad (5)$$

$$R_{vi2jn} = Z_{v2i} - (-1)^j \theta_{vy2i} \lambda_{vx3} + (-1)^n \theta_{vx2i} \lambda_{vy4} - V_{0i2jn} \quad (6)$$

$$R_{vi3jn} = Y_{v2i} - V_{0i3jn} + (-1)^j \theta_{vz2i} \lambda_{vx4} \quad (7)$$

$$R_{vi4jn} = Y_{v2i} - V_{0i4jn} + \theta_{vx2i} \lambda_{vz3} \quad (8)$$

$$R_{vi5jn} = Y_{v11} - Y_{v2i} - \theta_{vx11} \lambda_{vz1} + (-1)^i \theta_{vz11} \lambda_{vxi} \quad (9)$$

Therein,  $V_{0imjn}$  denotes the relative displacement of the bridge and surface roughness at the contact points of

wheel positions.

The equation of motion for a traveling monorail train on a bridge can be expressed as

$$\mathbf{M}_v \ddot{\mathbf{w}}_v + \mathbf{C}_v \dot{\mathbf{w}}_v + \mathbf{K}_v \mathbf{w}_v = \mathbf{f}_v, \quad (10)$$

where  $\mathbf{M}_v$ ,  $\mathbf{C}_v$  and  $\mathbf{K}_v$  respectively represent mass, damping and stiffness matrices of the train. In addition,  $\mathbf{f}_v$  is the interaction force vector applied on the train, and  $\mathbf{w}_v$  indicates the displacement vector of the train. Overdots represent the derivative with respect to time.

#### *Bridge model*

Equation (11) shows the equation of the forced vibration obtained for a bridge system under the moving monorail train:

$$\mathbf{M}_b \ddot{\mathbf{w}}_b + \mathbf{C}_b \dot{\mathbf{w}}_b + \mathbf{K}_b \mathbf{w}_b = \mathbf{f}_b, \quad (11)$$

where  $\mathbf{M}_b$ ,  $\mathbf{C}_b$  and  $\mathbf{K}_b$  respectively denote the mass, damping and stiffness matrices of the bridge. In addition,  $\mathbf{f}_b$  is an external force vector;  $\mathbf{w}_b$  indicates the displacement vector of the bridge. Rayleigh damping is adopted to form the damping matrix.

#### *Monorail bridge-train interaction model*

Considering the interaction force and wheel load at the contact points, the combination of Eqs. (10) and (11) gives the equation of the forced vibration for a monorail bridge-train interaction system as

$$\begin{bmatrix} \mathbf{M}_b & \mathbf{0} \\ \text{Sym.} & \mathbf{M}_v \end{bmatrix} \begin{Bmatrix} \ddot{\mathbf{w}}_b \\ \ddot{\mathbf{w}}_v \end{Bmatrix} + \begin{bmatrix} \mathbf{C}_{bb} & \mathbf{C}_{bv} \\ \text{Sym.} & \mathbf{C}_v \end{bmatrix} \begin{Bmatrix} \dot{\mathbf{w}}_b \\ \dot{\mathbf{w}}_v \end{Bmatrix} + \begin{bmatrix} \mathbf{K}_{bb} & \mathbf{K}_{bv} \\ \text{Sym.} & \mathbf{K}_v \end{bmatrix} \begin{Bmatrix} \mathbf{w}_b \\ \mathbf{w}_v \end{Bmatrix} = \begin{Bmatrix} \bar{\mathbf{f}}_b \\ \bar{\mathbf{f}}_v \end{Bmatrix}, \quad (12)$$

where  $\mathbf{C}_{bb}$ ,  $\mathbf{C}_{bv}$ ,  $\mathbf{K}_{bb}$  and  $\mathbf{K}_{bv}$  respectively indicate coupling damping and stiffness matrices of the bridge-train interaction system, which will be time-dependent when the train starts to move.  $\bar{\mathbf{f}}_b$  is the external load vector caused by the moving monorail train on a bridge.  $\bar{\mathbf{f}}_v$  is the dynamic wheel load vector of a train.

Validity of the monorail bridge-train interaction system is verified through comparison with field test data [2].

#### *Monorail bridge-train interaction model subjected to ground motion*

If the interaction system defined in Eq. (12) is subjected to ground motion, as would occur in an earthquake, then the problem is solvable by considering an additional force input because of acceleration of the mass

that is governed by an absolute coordinate.

The equation of motion for an interactive system under an earthquake in the simplified matrix is therefore

$$\begin{bmatrix} \mathbf{M}_b & \mathbf{0} \\ \text{Sym.} & \mathbf{M}_v \end{bmatrix} \begin{Bmatrix} \ddot{\mathbf{w}}_b \\ \ddot{\mathbf{w}}_v \end{Bmatrix} + \begin{bmatrix} \mathbf{C}_{bb} & \mathbf{C}_{bv} \\ \text{Sym.} & \mathbf{C}_v \end{bmatrix} \begin{Bmatrix} \dot{\mathbf{w}}_b \\ \dot{\mathbf{w}}_v \end{Bmatrix} + \begin{bmatrix} \mathbf{K}_{bb} & \mathbf{K}_{bv} \\ \text{Sym.} & \mathbf{K}_v \end{bmatrix} \begin{Bmatrix} \mathbf{w}_b \\ \mathbf{w}_v \end{Bmatrix} = \begin{Bmatrix} \bar{\mathbf{f}}_b - \ddot{a}_g \mathbf{M}_b \\ \bar{\mathbf{f}}_v - \ddot{a}_g \mathbf{M}_v \end{Bmatrix}, \quad (13)$$

where  $\ddot{a}_g$  is the ground acceleration at the basement of bridge structures during an earthquake.

## NUMERICAL MODELS

### *Monorail bridges*

The general layout and the basic geometry of advanced and conventional bridges are presented in Figure 3. Both bridges consist of two track girders with span lengths of 42.8 m. Steel bearings are adopted in the monorail bridges. The advanced bridge adopts composite steel girders with RC tramways, whereas the conventional bridge comprises steel girders. The mass of the superstructure of the advanced bridges is 200.56 tons and 146.32 tons for conventional bridges. Tables II and III respectively show properties of advanced and conventional bridges.

Figure 4 shows that bridges adopt steel piers made of SM490Y structural steel with the rectangle section. The pier is 15 m high. The cross-section is designed for Level-II ground motion with a low probability of occurrence according to the JRA code. The bridge footings of the models are idealized as springs. Table IV shows the spring constant used in the analysis. For the advanced bridge, the pier mass is 55.36 tons: 15.82 tons for the pier cap beam and 39.54 tons for the pier column. The pier's mass of the conventional bridge is 47.95 tons: 13.70 tons for the pier cap beam and 34.25 tons for the pier column.

Figure 5 shows the FE model for the bridges, which consist of two spans idealized by the beam element with 6 DOFs. It also incorporates a train's driving direction and observation points for displacement and shear force responses at the span center and the bearing supporting the G1 girder of the first span, respectively.

### *Ground motion*

Two kinds of ground motions, so called Level-I and Level-II ground motions, are adopted in the JRA code based on the seismic performance level of bridge structures. The Level-I ground motion is the moderate design ground motion, which has a return probability of once or twice in the service life of the structure. For the seismic performance under the Level-I ground motion both standard and important bridges should behave in an elastic manner without essential structural damage. The Level-II ground motion indicates the extreme design ground motion with low probability to occur, which is caused by plate boundary

earthquakes and inland earthquakes such as Kobe earthquake in 1995. For the seismic performance under the Level-II ground motion the standard bridges should prevent critical failure, while the important bridges should perform with limited damage.

The ground motion adopted in the seismic response analysis of monorail bridges is the Level-I ground acceleration of the JRA code [7]. Two accelerograms according to the soil sites shown in Figure 6 are used for analysis: the Group-I ground motion for the stiff soil site and the Group-II for the moderate soil site. The frequency in the legend of spectra is linked with the dominant frequency of each bridge response during earthquakes, as shown in the next section (Figures 8 and 9).

## **DYNAMIC RESPONSES OF MONORAIL BRIDGES AND TRAINS WITH GROUND MOTION**

Three numerical examples are used to investigate the effect of the train's dynamic system on seismic responses of steel monorail bridges under earthquakes. How the train is considered in the numerical example is shown in Figure 7 for the advanced bridge. The same concept is employed for the conventional bridge. The first one is the monorail bridge model without a train on the bridge (Figure 7(a)). Figure 7(b) shows that the second one is a model considering the train as an additional mass on the bridge model. It is noteworthy that the monorail train, during operation, is assumed to have the mass of 34.4 tons/car (= 26.7 tons/empty car + 129 passengers  $\times$  0.06 ton/person). Figure 7(c) shows a third situation that illustrates the interaction between a bridge and stationary train. The bridge-moving train interaction model shown in Figure 7(d) is used to investigate the seismic response under the moving monorail train. The target speed is 3.9 m/s, which is the speed that the first car in the monorail train, composed of six cars, can travel the observed bridge during Group-I ground motion of 25 seconds. Half of the mass of the adjacent girder is considered in the analysis, as shown in Figure 7 to incorporate the inertia effect of the neighboring span: 50.14 tons and 36.58 tons for advanced and conventional bridges, respectively.

The dynamic response of each bridge is obtained by summing up to the mode related to the frequency near 30 Hz: for the model ignoring the train's mass, up to the 50th (29.8 Hz) and 40th (29.4 Hz) modes were shown for advanced and conventional bridges respectively; up to the 57th (29.7 Hz) and 46th (29.4 Hz) modes were considered respectively in advanced and conventional bridges for the model considering the train as an additional mass. Newmark's  $\beta$  method [10] is adopted to solve simultaneous differential equations of the monorail bridge-train interaction system under earthquakes. The value of 0.25 is adopted for  $\beta$  to obtain stable and accurate solutions. The damping constant of the monorail bridge during an earthquake is assumed as 5%.

### *Eigenvalue analysis*

Eigenvalue analyses were carried out to gain fundamental insight into the dynamic characteristics of the bridges. Mode shapes and natural frequencies of the first five modes are listed in Table V. That table shows that the first natural frequencies are 1.33 Hz and 1.54 Hz, respectively, for the advanced and conventional

bridge models without considering the train's mass. Those values are 1.09 Hz and 1.15 Hz for each bridge model considering the train as an additional mass. The natural frequencies in the parenthesis of Table V are values taken from considering the train's mass as an additional mass on the bridge. The first three modes are in relation to the lateral bending of steel piers coupled with that of the track girders'. The vertical bending modes of the track girders appear in the fourth and fifth modes.

#### *Dynamic response of the bridges*

The seismic responses of respective bridges are investigated as shown in Figure 8 to Figure 11, where the displacement response of the first span center is summarized in Figures 8 and 9 according to ground motion. The shear force at the observation with the ground motion is shown in Figures 10 and 11. Bridge responses under traveling trains are also shown in each figure to provide information about the seismic responses of bridges under moving trains. A noteworthy point here is that the model considering a traveling train subsumes that the train starts to move and enter the bridge at the instant that an earthquake occurs, while the model of a stationary train is affected by the six cars of the monorail train during an earthquake. For that reason, it is difficult to compare the seismic responses of bridges interacting with the stationary train with responses for a moving train, as shown in Figures 8–11.

As illustrated in Figures 8–9, both the absolute peak and RMS values of the displacement response of the advanced bridge are greater than those of the conventional bridge with both ground motions. It indicates that the advanced bridge with fewer lateral members and heavier track-girders than those of the conventional bridge is easily vibrated in the transverse direction during earthquakes. Considering the effect of the train mass on bridges as summarized in Figures 8(b) and 9(b), determining the train on bridges provides greater seismic response than that with the model without the train shown in Figures 8(a) and 9(a) because of the additional inertial effect of the train on bridges during earthquakes. Noteworthy results are that the model that incorporates train dynamics (Figures 8(c), 8(d), 9(c) and 9(d)) tends to show less seismic response than that which ignores the dynamic system of the train as shown in Figures 8(b) and 9(b). They demonstrate that the bridge model considering the train as an additional mass provides a conservative design.

Fourier amplitudes of displacement responses show that the bridge models that ignore the monorail train are affected strongly by the dynamic component near 1.34 Hz and 1.49 Hz under the Group-I ground motion for the advanced and conventional bridges, respectively. Similarly, under the Group-II ground motion, 1.37 Hz and 1.49 Hz are dominant frequencies for the advanced and conventional bridges, respectively. Those strong effects pertain because of the effect of the first natural frequency of each bridge summarized in Table V (1.33 Hz and 1.54 Hz, respectively, for the advanced and conventional bridge models without considering train's mass; 1.09 Hz and 1.15 Hz, respectively, for the advanced and conventional bridge models considering the train as an additional mass) together with the dynamic component in relation to those frequencies shown in each accelerogram of Figure 6. On the other hand, the Fourier amplitudes of the bridge models considering the train's mass and the train as a dynamic system as

shown in Figures 8(b) to 8(d) as well as in Figures 9(b) to 9(d) demonstrate that the bridge response tends to respond with lower dominant frequencies that are attributable to the increased mass of an external load such as a monorail train.

It is noteworthy that, as stated in Eq.(12), the coefficient matrices  $C_{bb}$ ,  $C_{bv}$ ,  $K_{bb}$ ,  $K_{bv}$  and wheel load vector ( $\bar{f}_b$ ) in Eq.(13) are affected by train's spring and damping constants as well as the train's position at a time. It indicates that those matrices are time-variant when the train starts to move. On the other hand, when the stationary train is on the bridge, those coefficients are time-invariant. Therefore bridge responses under the moving train differ from those responses under the stationary train.

Shear force at the observation bearing during earthquakes is summarized in Figures 10 and 11 according to ground motions. The effects of the bridge type and a train on the shear force at the bearing are similar to the tendency observed in the seismic displacement response of the bridge.

This study also examines the reason why the seismic response of the monorail bridge that incorporates the bridge-train interaction tends to be lower than the response of the bridge model that incorporates the train as an additional mass on a bridge. Figure 12, which shows the behavior of the advanced monorail bridge and train at the times of 11.8 s and 12.2 s under Group-II ground motion, answers that question. The existence of phase between train and bridge systems in ground motion is observed in Figure 12. As shown in Figure 12(a), the upper part of the train (train body) remains on the right part, whereas the bridge completely deforms to the left-hand side at 11.8 s; a reverse tendency is visible in Figure 12(b).

It clearly illustrates that the dynamic system of the train might act as a damper during earthquakes. Observations show that the phase difference depending on dynamic characteristics of the monorail train and bridge system helps to reduce the inertia effect during earthquakes.

#### *Dynamic response of train*

The straddle-type monorail bridge consists of elevated narrow track girders. Passengers in a straddle-type monorail train feel closer to an open space and thereby become more sensitive to vibration with a visual connection than do passengers in a railway train or a vehicle on elevated viaducts. The dynamic response of a monorail train on a monorail bridge under ground motion is examined next.

Figures 13 and 14 show the respective acceleration responses taken from the train's body under Group-I and Group-II ground motions. The observation point during the train traveling with ground motion is the floor on the front axle of the first car. The floor on the rear axle of the second car positioned on the center of the second span is the observation point for the train standing on the bridge. Acceleration responses of the monorail train on the advanced bridge are slightly greater than those of the train on the conventional bridge under earthquakes.

## **CONCLUSIONS**

Seismic response analyses of advanced and conventional monorail bridges were undertaken to investigate

the effect of the dynamic system of a monorail train on the bridge responses under the Level-I ground motions specified in the JRA code. Dynamic responses of monorail trains on monorail bridges with ground motions were also examined. Some important conclusions can be summarized as follows:

- 1) Seismic responses of the advanced bridge, such as the displacement at the span center and the shear force at the bearing, are greater than those of the conventional bridge because of the heavier girder weight and less lateral bracing of the advanced bridge than of the conventional bridge. This fact emphasizes the need for detailed inspection of seismic performance for advanced bridges under extreme ground motion, which dominates the seismic design.
- 2) The model that incorporates train dynamics tends to reduce the seismic response in comparison with the bridge model considering the train as an additional mass. One reason for that phenomenon is that the phase difference depending on dynamic characteristics of the monorail train and bridge system helps to reduce the inertia effect during earthquakes.
- 3) Consideration of the dynamic interaction between the bridge and train during seismic design can provide an economic design under the ground motions specified in the JRA code. In other words, existing design methods, which consider the train as an additional mass, provide a conservative result.
- 4) Acceleration responses of monorail trains on advanced bridges are slightly greater than those of trains on conventional bridges under earthquakes.

It is difficult to say, however, that the code specified ground motions are appropriate to examine even the train response because the code specified ground motions are directly connected with the seismic design and response of bridge structures. Future study needs, therefore, further investigations using various seismic records to make a general conclusion for the train dynamics on the seismic response of bridges.

#### ACKNOWLEDGMENTS

This study is supported by the Japan Society of the Promotion of Science (Grant-in-Aid for Scientific Research (B) under project No. 17360213) which is gratefully acknowledged. The authors are also grateful to Mr. T. Kanbara, a former graduate student of Osaka University of Japan, for his help in designing the steel piers. Additional thanks go to Mr. F. Taniguchi, a graduate student of Kobe University of Japan, for his assistance in the simulation.

#### REFERENCES

1. Lee CH, Kim CW, Kawatani M, Nishimura N, Kamizono T. Dynamic response analysis of monorail bridges under moving trains and riding comfort of trains. *Engineering Structures* 2005; **27/14**: 1999-2013.
2. Lee CH, Kawatani M, Kim CW, Nishimura N, Kobayashi Y. Dynamic response of a monorail under a moving train. *Journal of Sound and Vibration*. (accepted for publication)

3. Kameda H, Murono Y, Nanjou A, Sasaki N. Earthquake response of highway bridges under bridge-vehicle system. *Journal of Structural Mechanics and Earthquake Engineering* (JSCE) 1999; **626/I-48**: 93-106. (in Japanese)
4. Yang YB, Wu YS. Dynamic stability of trains moving over bridges shaken by earthquakes. *Journal of Sound and Vibration* 2002; **258**: 65-94.
5. Miyamoto T, Ishida H, Matsuo M. Running safety of railway vehicle as earthquake occurs. *QR of RTRI* 1997; **38/3**: 117-122.
6. Maruyama Y, Yamazaki F. Seismic response analysis on the stability of running vehicles. *Earthquake Engineering and Structural Dynamics* 2002; **31**: 1915-1932.
7. Japan Road Association. *Specifications for Highway Bridges, Part V: Seismic Design*. JRA: Tokyo, Japan, 2002.
8. Guyan RJ. Reduction of stiffness and mass matrices. *AIAA J* 1965; **3**(2): 380.
9. Kim CW, Kawatani M, Kim KB. Three-dimensional dynamic analysis for bridge-vehicle interaction with roadway roughness. *Computers and Structures* 2005; **83**: 1627-1645.
10. Newmark NM. A Method of computation for structural dynamics. *J. of Eng. Mech. Div.* (ASCE) 1970; **96**: 593-620.

Table I. Monorail car properties: no passengers.

Parameter		Notation	Value
Mass (ton)	Body	$m_{v11}$	14.22
	Bogie	$m_{v21}(=m_{v22})$	6.20
Spring constant (kN/m)	Air suspension (vertical)	$K_{v1111}(=K_{v1112}=K_{v2111}=K_{v2112})$	900.0
	Traveling wheels	$K_{v1211}(=K_{v1212}=K_{v1221}=K_{v1222}=K_{v2211}=K_{v2212}=K_{v2221}=K_{v2222})$	5170.0
	Steering wheels	$K_{v1311}(=K_{v1312}=K_{v1321}=K_{v1322}=K_{v2311}=K_{v2312}=K_{v2321}=K_{v2322})$	6370.0
	Stabilizing wheels	$K_{v1411}(=K_{v1412}=K_{v2411}=K_{v2412})$	6370.0
	Air suspension (lateral)	$K_{v1511}(=K_{v2511})$	980.0
Damping coefficient (kN·s/m)	Air suspension (vertical)	$C_{v1111}(=C_{v1112}=C_{v2111}=C_{v2112})$	22.8
	Traveling wheels	$C_{v1211}(=C_{v1212}=C_{v1221}=C_{v1222}=C_{v2211}=C_{v2212}=C_{v2221}=C_{v2222})$	26.1
	Steering wheels	$C_{v1311}(=C_{v1312}=C_{v1321}=C_{v1322}=C_{v2311}=C_{v2312}=C_{v2321}=C_{v2322})$	185.5
	Stabilizing wheels	$C_{v1411}(=C_{v1412}=C_{v2411}=C_{v2412})$	185.5
	Air suspension (lateral)	$C_{v1511}(=C_{v2511})$	333.6
Geometry (m)		$\lambda_{vx1}(=\lambda_{vx2})$	4.80
		$\lambda_{vx3}$	0.75
		$\lambda_{vx4}$	1.25
		$\lambda_{vy1}$	1.490
		$\lambda_{vy2}$	1.025
		$\lambda_{vy3}$	0.7823
		$\lambda_{vy4}$	0.2
		$\lambda_{vz1}$	0.885
		$\lambda_{vz2}$	0.630
		$\lambda_{vz3}$	1.085

Table II. Monorail bridge properties: advanced bridge.

Property		Steel girder (SM490Y)	RC slab	End crossbeam (SM400)	Crossbeam (SM400)	Lateral bracing (SM400)
Numbers		2	-	2	7	32
Young's modulus (GPa)		205	45	205	205	205
Upper flange	width (mm)	640	850	300	300	-
	thickness (mm)	13	415 (depth)	28	24	-
Web plate	depth (mm)	2385	-	844	652	176
	thickness (mm)	11	-	16	13	8
Lower flange	width (mm)	640	-	300	300	200
	thickness (mm)	25	-	28	24	12
Yield stress (MPa)		353	45	235	235	235

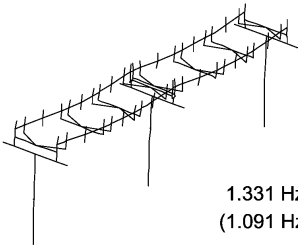
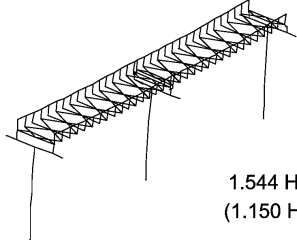
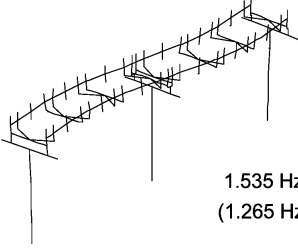
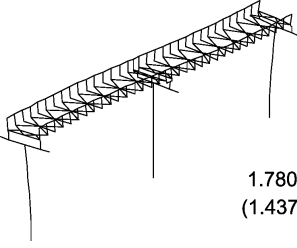
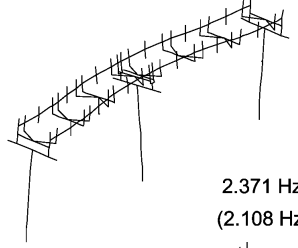
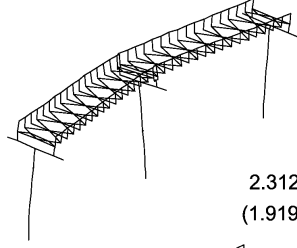
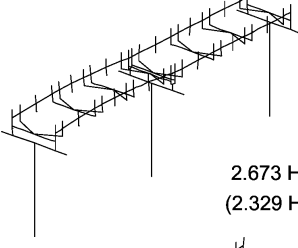
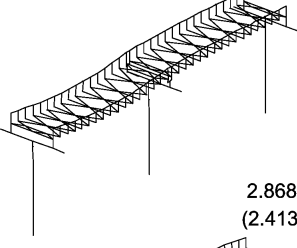
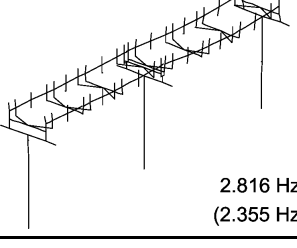
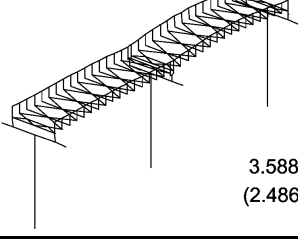
Table III. Monorail bridge properties: conventional bridge.

Property		Steel track girder (SM490Y)	End crossbeam (SM400)	Crossbeam (SM400)	Lateral bracing (SM400)
Numbers		2	2	2	8
Young's modulus (GPa)		205	205	205	205
Upper flange	width (mm)	690	300	320	-
	thickness (mm)	18	22	19	-
Web plate	depth (mm)	2782	844	681	134
	thickness (mm)	11	11	9	12
Lower flange	width (mm)	840	300	320	204
	thickness (mm)	19	22	19	10
Yield stress (MPa)		353	235	235	235

Table IV. Spring constant of foundation.

Vertical spring (kN/m)	3,581,400
Lateral spring (kN/m)	28,275,000
Rotational spring (kN·m/rad)	1,003,300

Table V. First five natural modes and frequencies of monorail bridges.

Mode No.	Advanced bridge	Conventional bridge
1	 1.331 Hz * (1.091 Hz) **	 1.544 Hz * (1.150 Hz) **
2	 1.535 Hz * (1.265 Hz) **	 1.780 Hz * (1.437 Hz) **
3	 2.371 Hz * (2.108 Hz) **	 2.312 Hz * (1.919 Hz) **
4	 2.673 Hz * (2.329 Hz) **	 2.868 Hz * (2.413 Hz) **
5	 2.816 Hz * (2.355 Hz) **	 3.588 Hz * (2.486 Hz) **

\* Disregarding the train's mass and \*\* Considering train's mass.

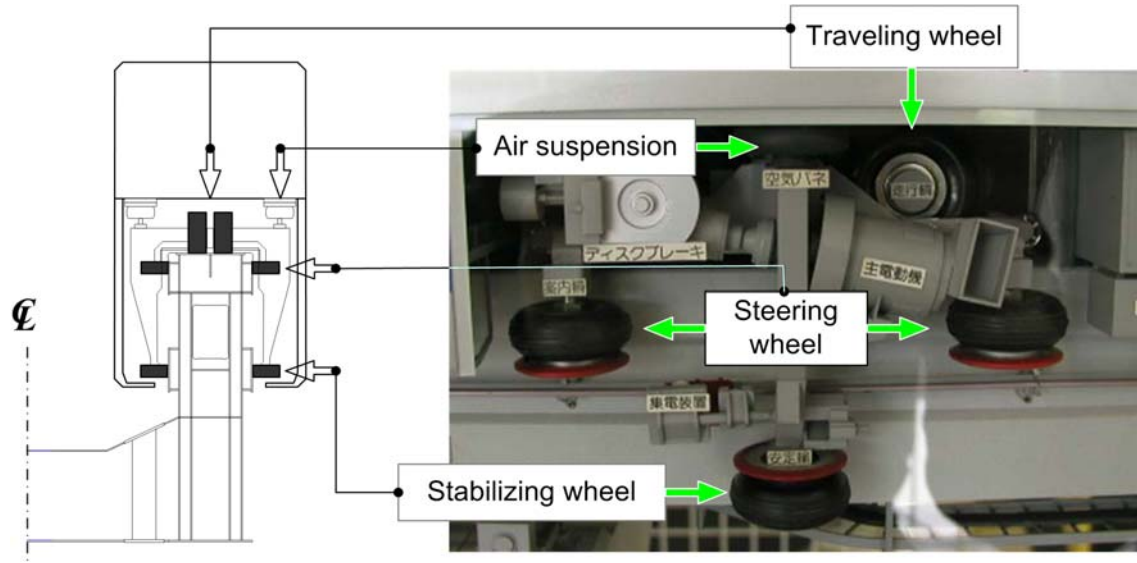


Figure 1. Configuration of straddle-type monorail train on the track girder.

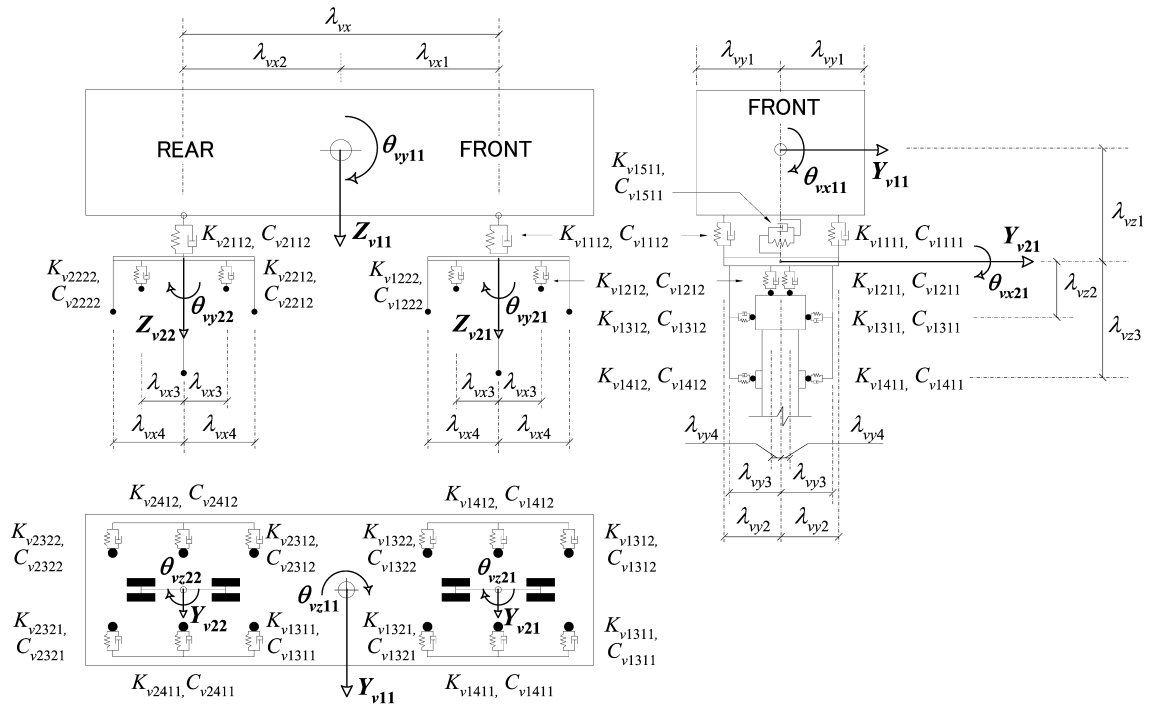


Figure 2. Idealized monorail car of 15 DOFs.



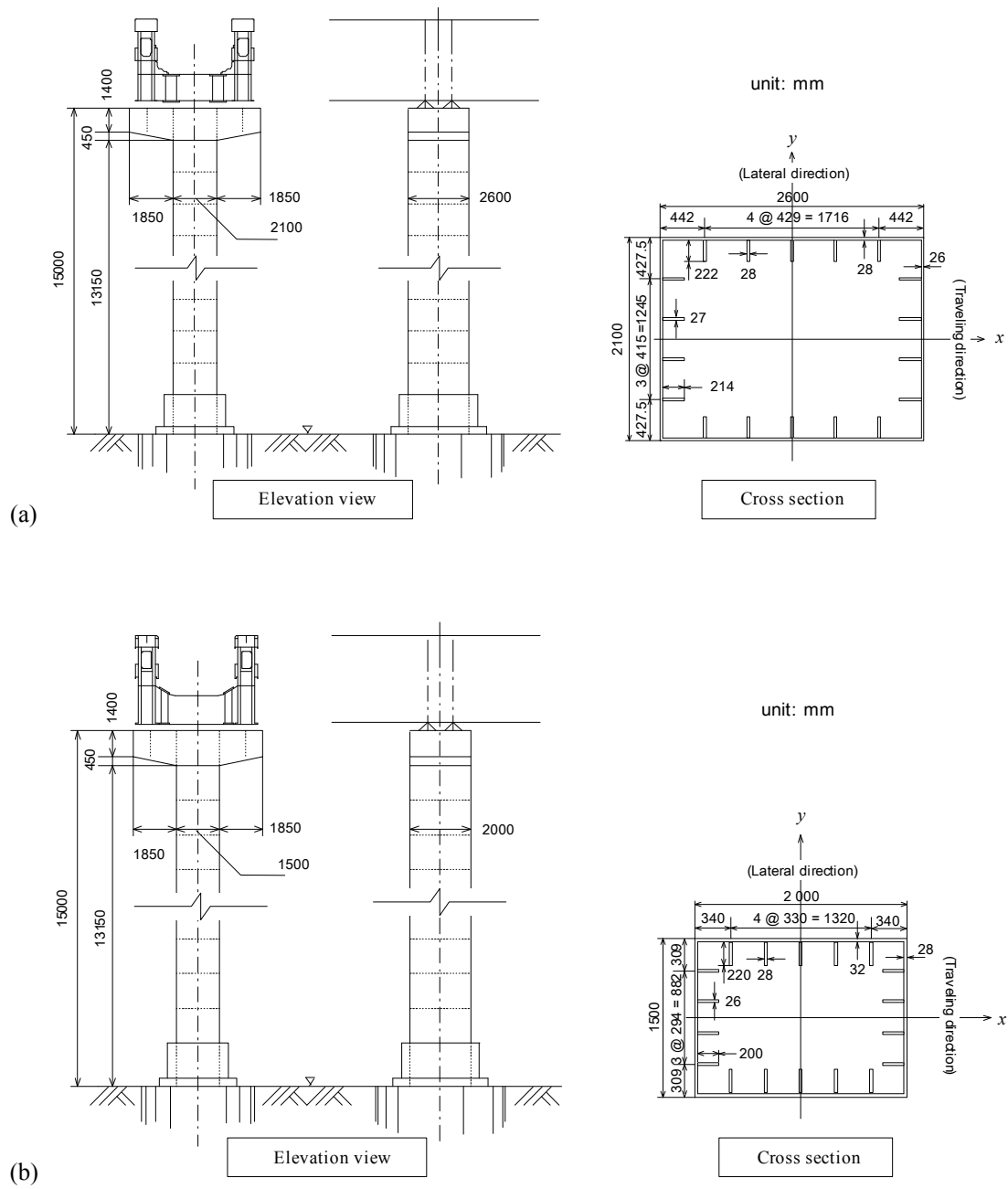


Figure 4. Configuration of steel piers: (a) advanced bridge; and (b) conventional bridge.

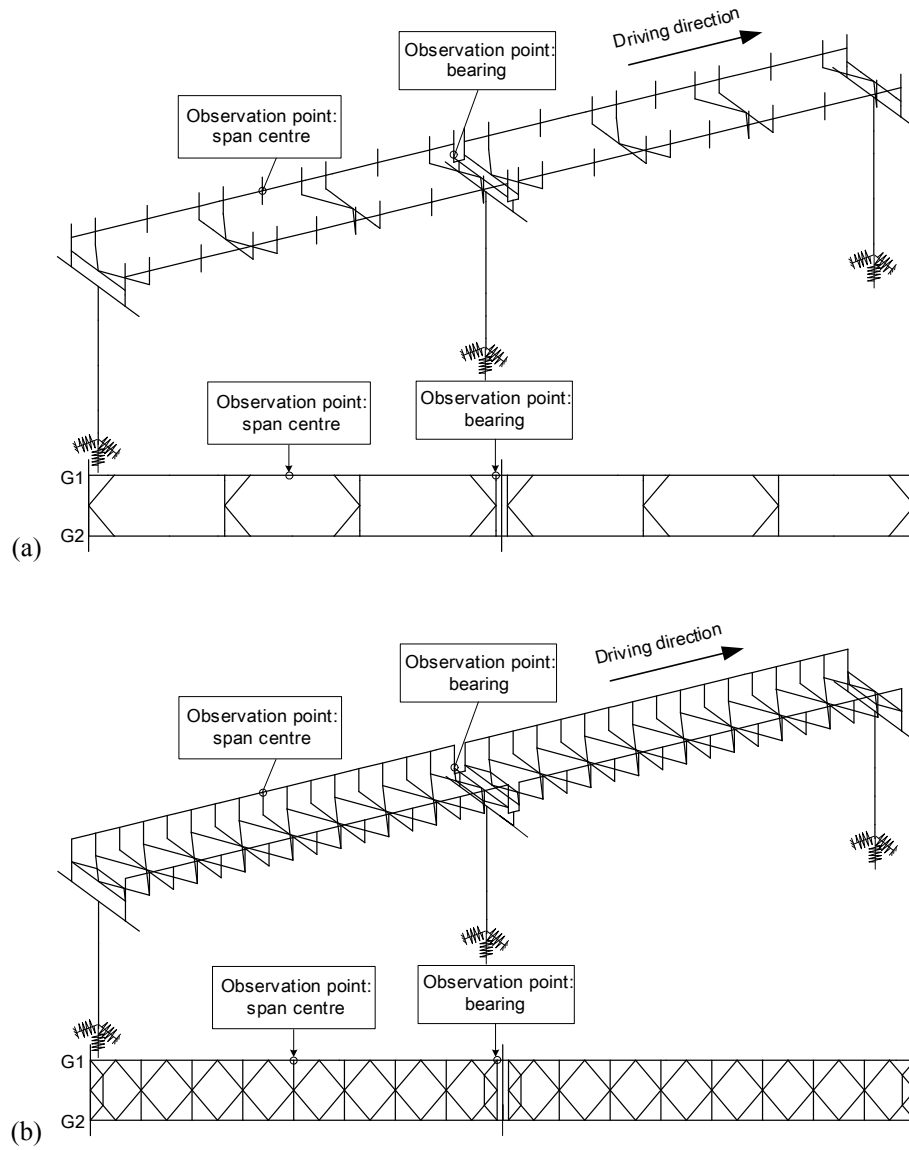


Figure 5. FE models of monorail bridges: (a) advanced bridge; and (b) conventional bridge.

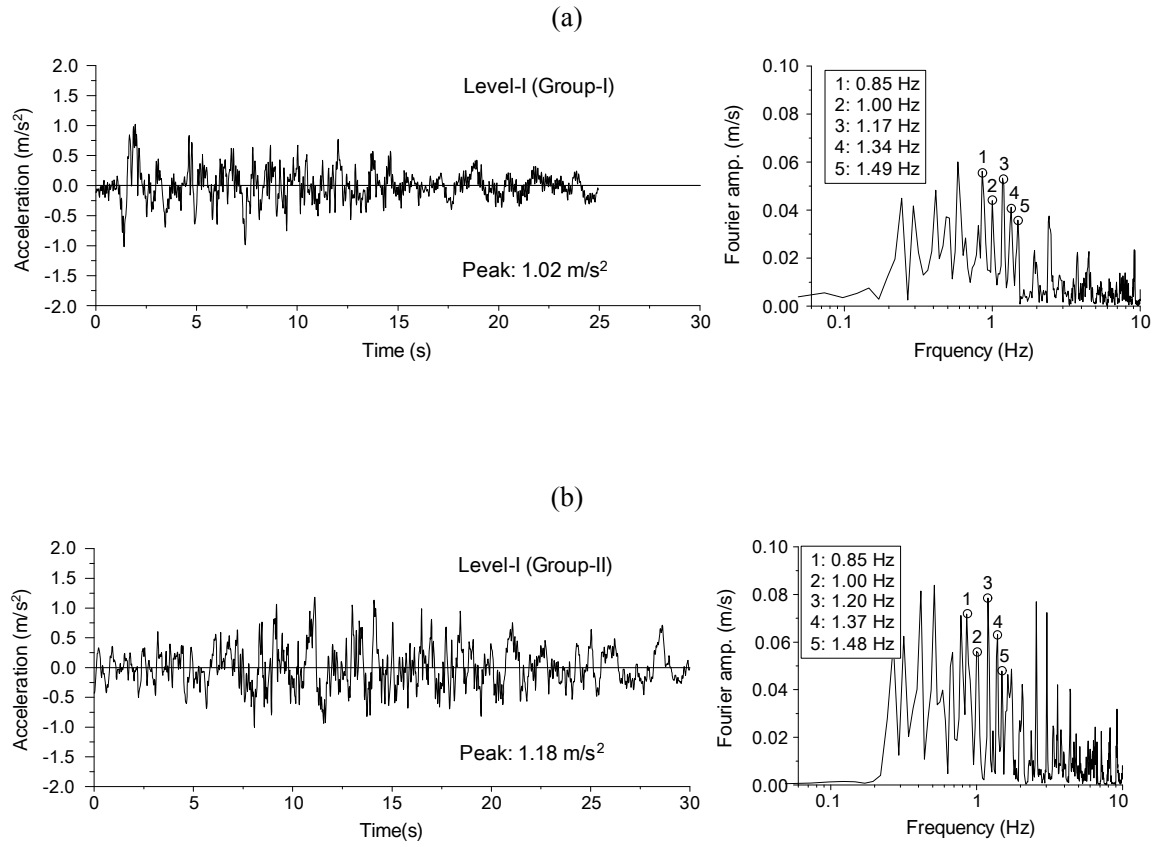


Figure 6. Accelerograms of JRA code (Level-I) and Fourier amplitude of acceleration: (a) stiff soil site (Group-I); and (b) moderate soil sites (Group-II).

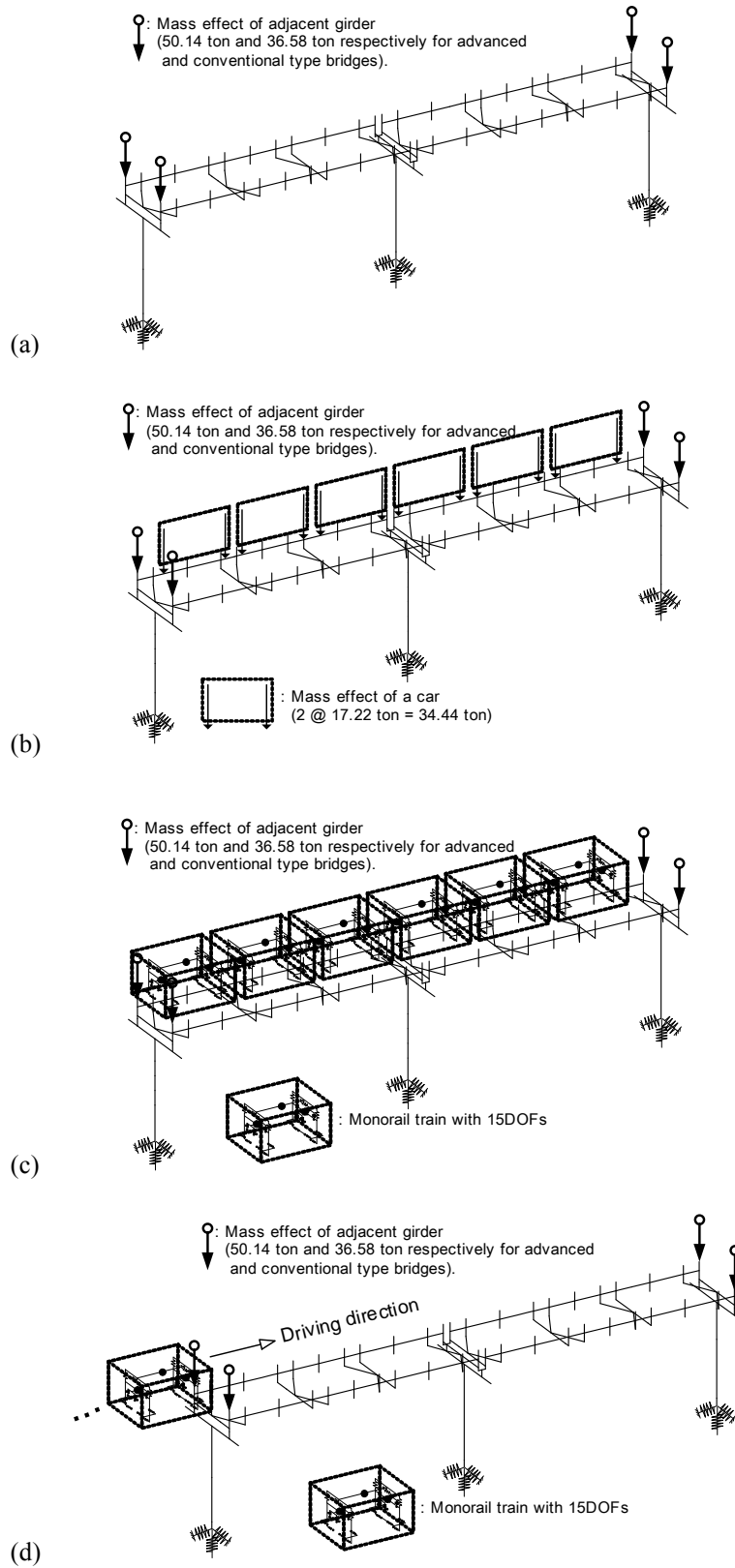


Figure 7. Models for numerical example: (a) disregarding the train's mass; (b) considering the train's mass; (c) considering bridge-stationary train interaction; and (d) considering bridge-moving train interaction.

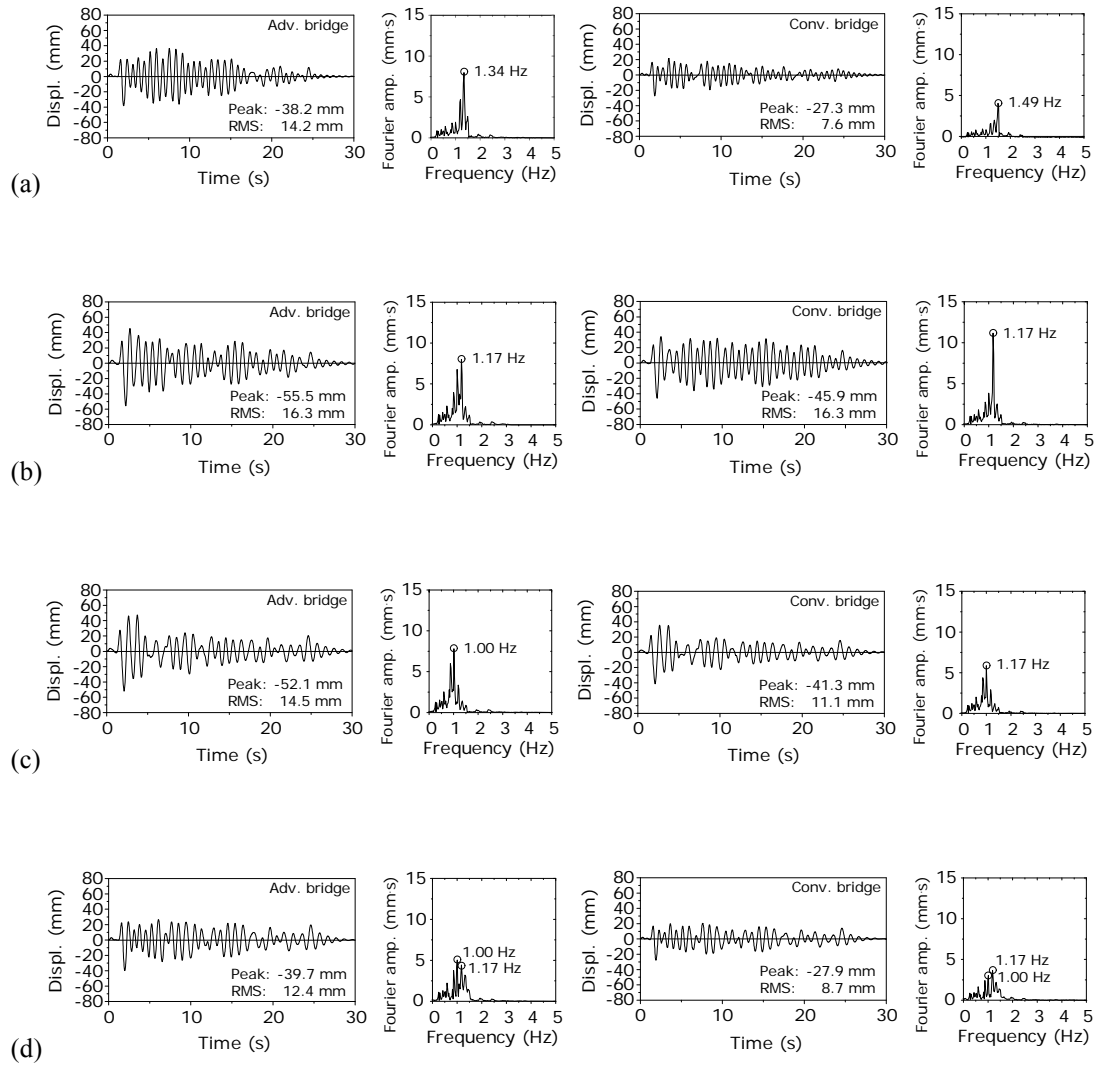


Figure 8. Lateral displacement at the first span center under Group-I ground motion and Fourier amplitude of displacement of monorail bridges: (a) model disregarding the train; (b) model with the train considered as an additional mass; (c) model considering interaction between the bridge and a stopped train; and (d) model considering interaction between the bridge and a moving train ( $v = 3.9$  m/s).

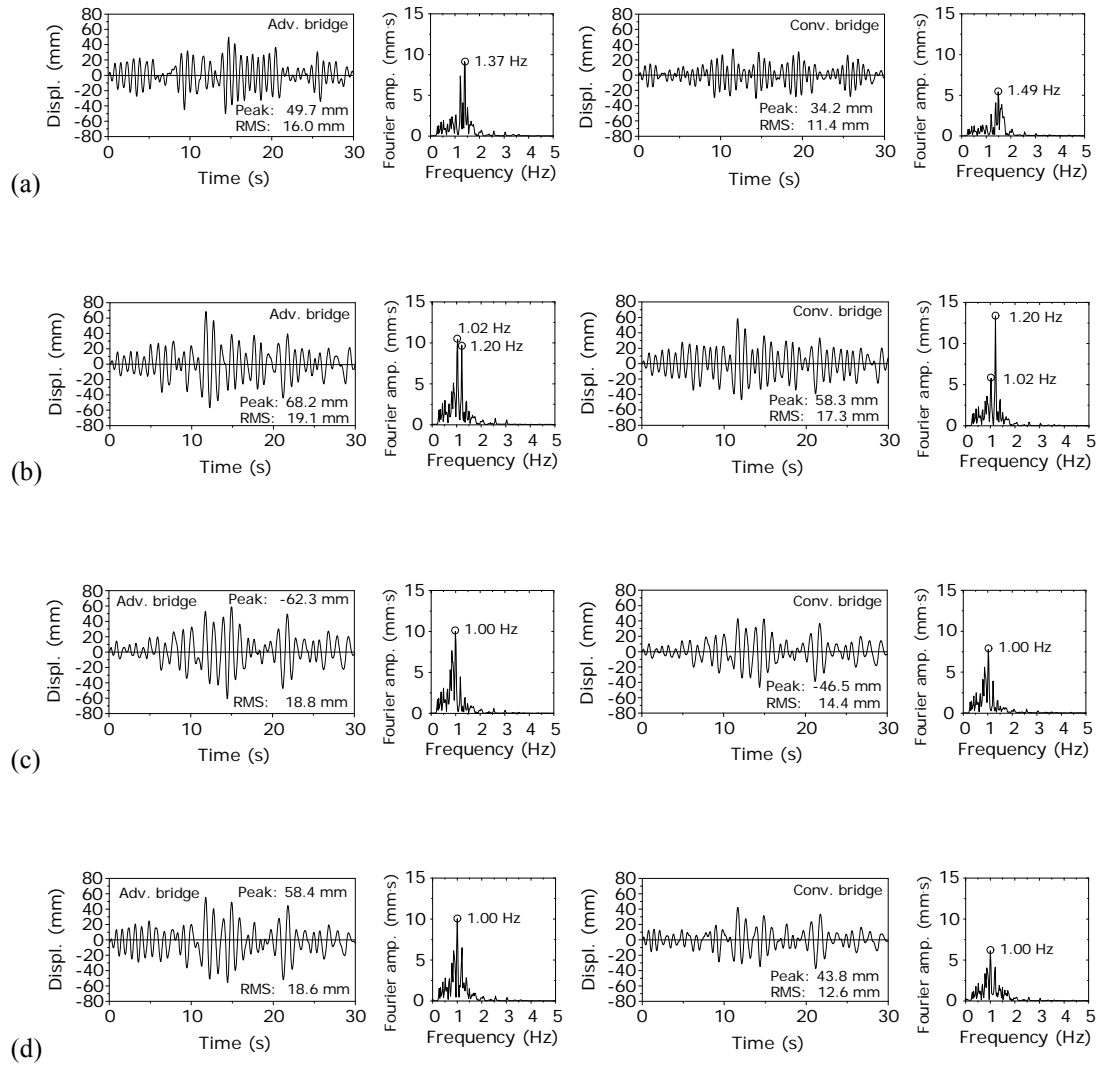


Figure 9. Lateral displacement at the first span center under Group-II ground motion and Fourier amplitude of displacement of monorail bridges: (a) model disregarding the train; (b) model with the train considered as an additional mass; (c) model considering interaction between the bridge and a stopped train; and (d) model considering interaction between the bridge and a moving train ( $v = 3.9$  m/s).

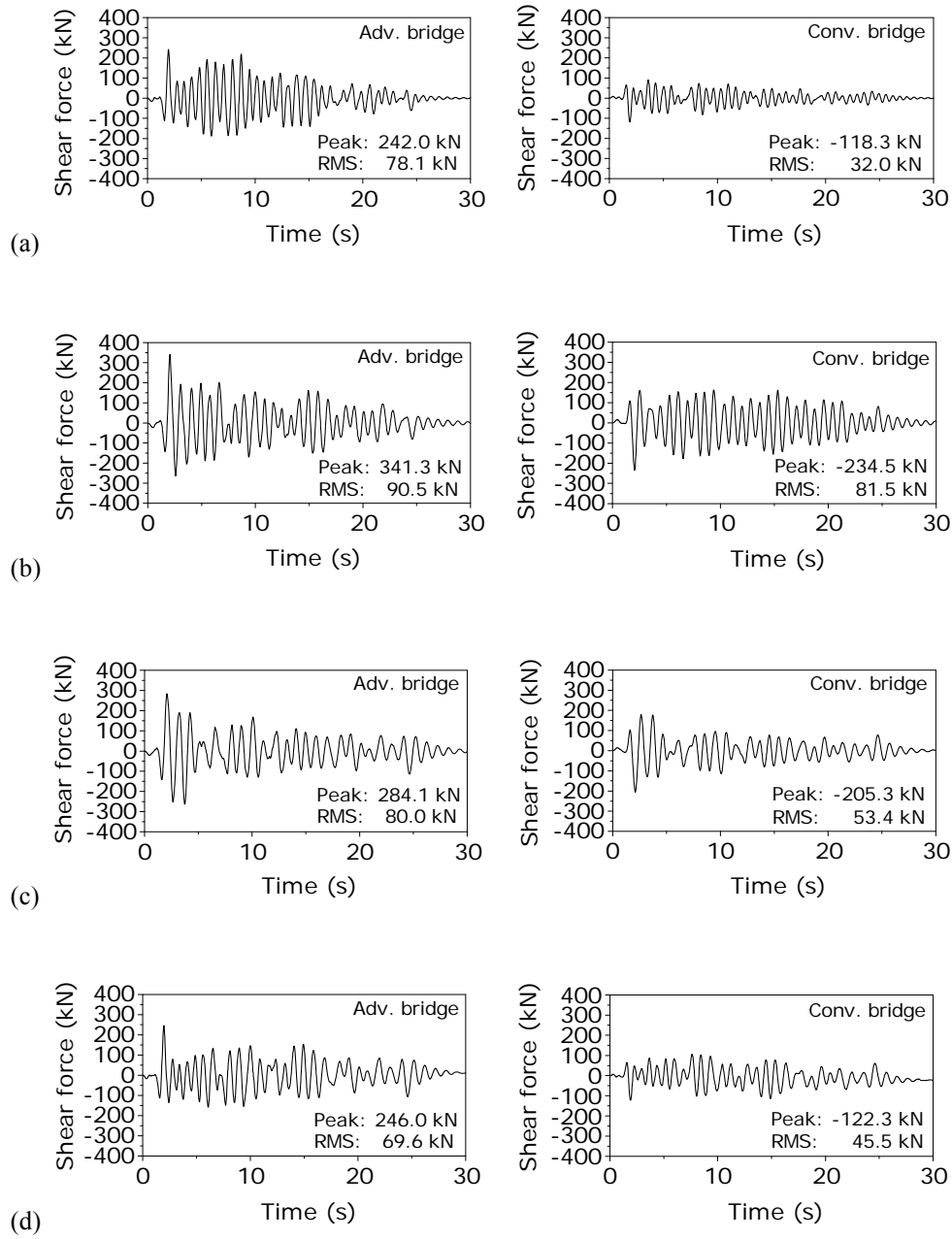


Figure 10. Shear force at the bearing of numerical models under Group-I ground motion: (a) model disregarding the train; (b) model with the train considered as an additional mass; (c) model considering interaction between the bridge and a stopped train; and (d) model considering interaction between the bridge and a moving train ( $v = 3.9$  m/s).

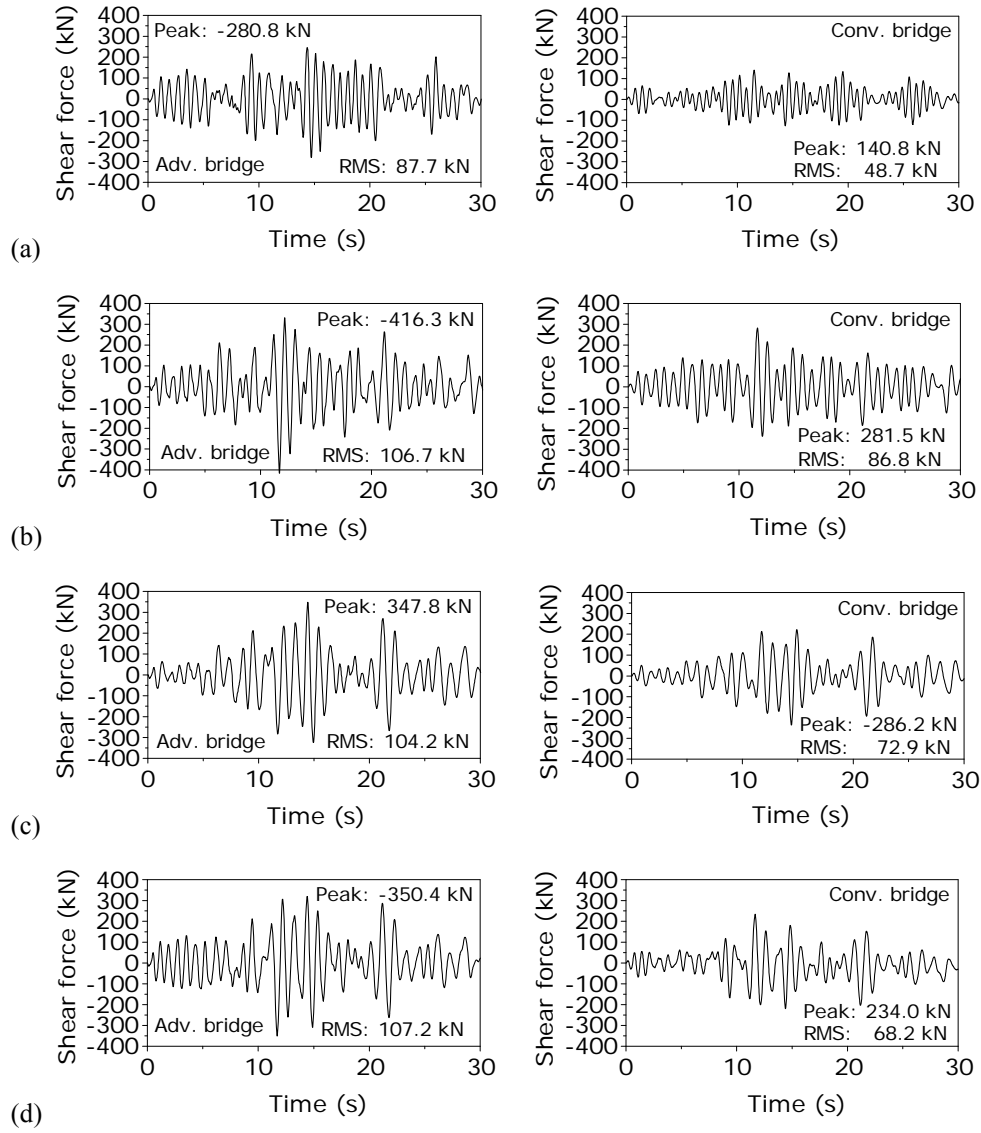


Figure 11. Shear force at the bearing of numerical models under Group-II ground motion: (a) model disregarding the train; (b) model with the train considered as an additional mass; (c) model considering interaction between the bridge and a stopped train; and (d) model considering interaction between the bridge and a moving train ( $v = 3.9$  m/s).

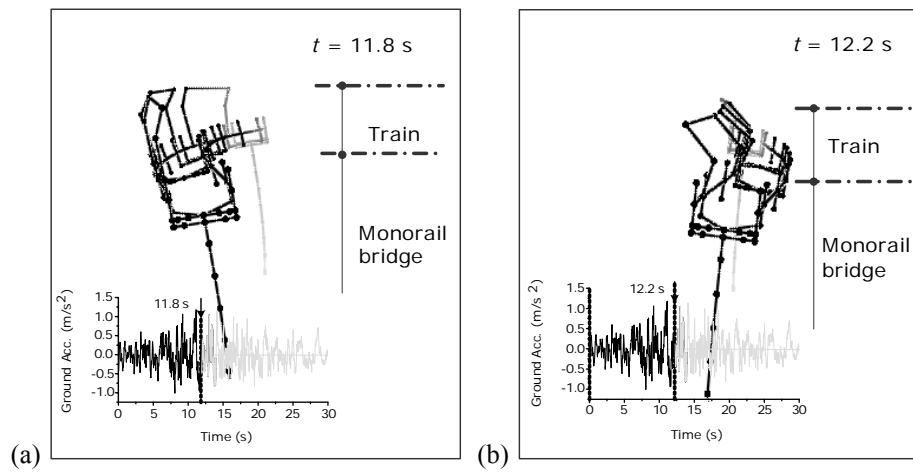


Figure 12. Phase motion of monorail train and bridge under Group-II ground motion: (a) at time  $t=11.8 \text{ s}$ ; and (b) at time  $t=12.2 \text{ s}$ .

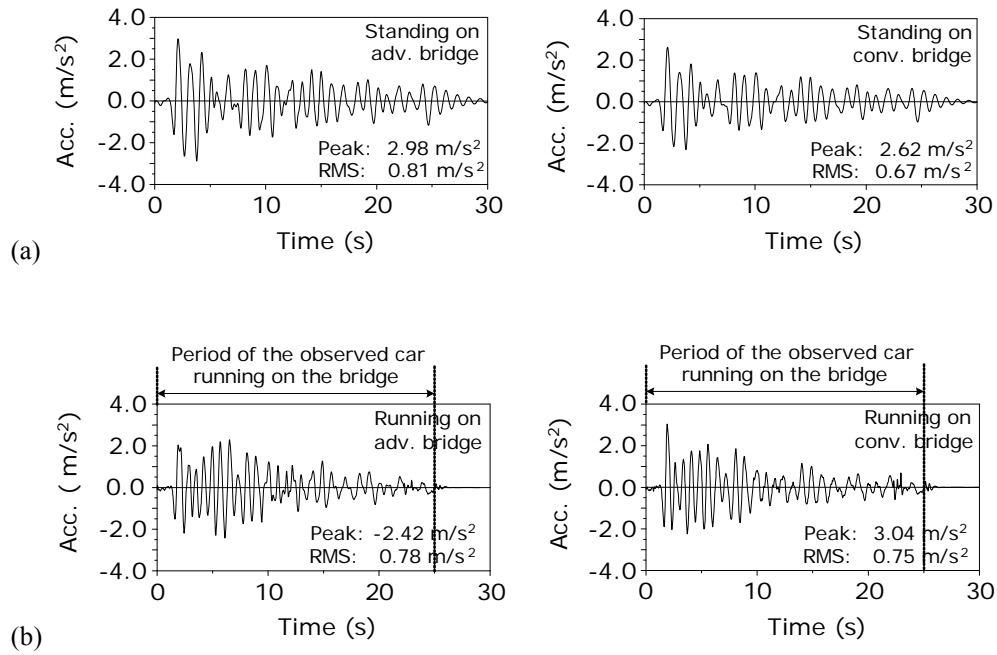


Figure 13. Acceleration of the observation car on monorail bridges under Group-I ground motion: (a) floor on the rear axle of the second car of the train standing on a bridge; and (b) floor on the front axle of the head car of the train running on a bridge ( $v = 3.9$  m/s).

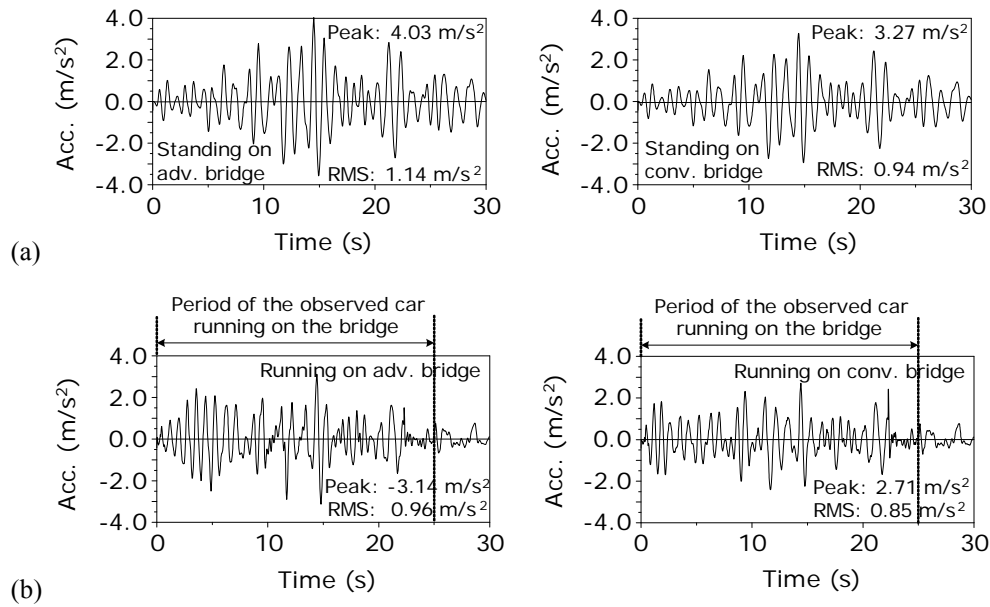


Figure 14. Acceleration of the observation car on monorail bridges under Group-II ground motion: (a) floor on the rear axle of the second car of the train standing on a bridge; and (b) floor on the front axle of the head car of the train running on a bridge ( $v = 3.9$  m/s).